Research Article

Design of a cable-driven parallel robot for landmine detection

Assylbek Jomartov[1] · Amandyk Tuleshov[1] · Aziz Kamal[1] · Azizbek Abduraimov[1]

Received: 24 October 2022 / Accepted: 13 October 2023
Published online: 24 October 2023

Abstract
A cable-driven parallel robot (CDPR) for landmine detection, mounted on a vehicle is developed in this work. In the CDPR, the end effector (EE) is suspended on flexible cables, in contrast to the rigid links in traditional parallel robots. Compared to traditional parallel robots, the CDPR have lower inertial characteristics and higher payload-to-weight ratio, resulting in a high speed. The CDPR for landmine detection operates in search mode, lowers the end EE to the possible lower position and the metal detector scanning the minefield. After scanning the area of the minefield, limited by the workspace of the CDPR in the X, Y plane, the information received is transmitted to the sappers. Tests of a prototype of a CDPR for landmine detection showed good performance of its work for detecting landmine.

Article highlights

- A scheme of the cable-driven parallel robot for landmine detection, installed on vehicle, is developed.
- The prototype of cable-driven parallel robot for landmine detection is made and tested in laboratory.
- The operation of cable-driven parallel robot for landmine detection is improved, due to the use of a smooth periodic function, for the end effector trajectory.

Keywords Cable-driven parallel robot · Landmine detection · Tension control · Stepped trajectory · Metal detector · Prototype

1 Introduction

Minefields are created during military conflicts pose a serious threat to the civilian population. Landmine is an effective, cheap weapon and consists of a trigger mechanism, detonator and an explosive in a metal (plastic) case. Mining is an inexpensive and simple operation, while demining is a complex, dangerous, expensive and slow operation due to their unknown location.

The manual method of demining is still the most common. If only the manual method is used, then it will take hundreds of years of work for sappers to demine minefields. In this regard, the development of robots for landmine detection and its demining has become an urgent task [1]. At present, many methods and technologies have been developed for landmine detection [2]. However, the effectiveness of available landmine detection technologies depends on the terrain and soil composition, vegetation content, landmine size and design. The use of robots increases the speed of detecting and demining of the minefields by automating the process [3]. Robots increase safety and efficiency of sappers. Robots speed up clearance process and are very useful for quick checking of an area for landmines.

The following works are devoted to the development and research of robots for detecting landmines: walking

✉ Assylbek Jomartov, assylbekjomartov@gmail.com | [1]Joldasbekov Institute of Mechanics and Engineering, Almaty 050010, Kazakhstan.

robots for demining [4–7], robots installed on wheeled vehicles [8], robots installed on tracked vehicles [9]. The Tokyo Institute of Technology has developed a semi-autonomous landmine detection robot called Gryphon (Fig. 1); [10]. It consists of a vehicle-mounted robotic arm capable of scanning minefield and providing accurate images of location of landmines over an area of 2 square meters. An operator, located remotely, monitors the scanning process and marks suspicious places using GPS coordinates or marking device. The disadvantage of this robot is the small scanning area of the minefield.

At the University of Florida, the Machine Intelligence Laboratory (MIL) created the MILmine Sweeper robot (Fig. 2) to detect and mark landmines. The detection of mines is carried out through the use of a mine detector and marking of mines is carried out with spray paint when a mine is detected. The MILmine Sweeper robot has limited mobility and is not suitable for rough terrain.

The Robotics Institute at Carnegie Mellon University has developed the sapper robot Finder (Fig. 3). The Finder is equipped with 16 ultrasonic sensors for detecting and avoiding obstacles, as well as a positioning device. The Finder robot is equipped with a standard metal detector. Robot Finder can only work on plane terrain without vegetation and other environmental obstructions.

The Shrimp III robot was developed at the Autonomous Systems Laboratory (ASL) of EPFL-Switzerland (Fig. 4). This version is equipped with 6 motors built into the wheels and is controlled by two servos and can turn on the spot. The Shrimp III robot can be used in demining operations on rough terrain [11]. The disadvantage of this robot is a small scanning area of minefield.

Chiba University, Japan has developed a six-legged robot COMET equipped with several sensors for detecting mines (Fig. 5). The weight of the robot is 990 kg, the length is 4 m, the width is 2.5 m and the height is 0.8 m. The robot can move at a speed of 300 m per hour in the detection mode on various terrains [12]. The disadvantages

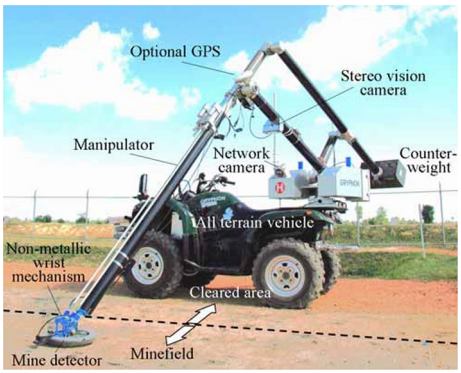

Fig. 1 Semi-autonomous landmine detection robot Gryphon

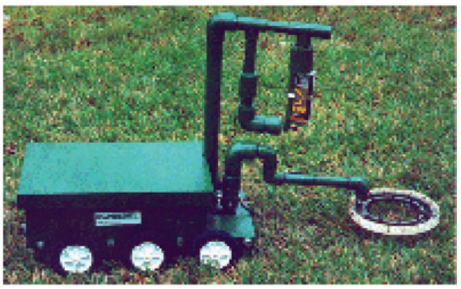

Fig. 2 MILmine Sweeper robot

of the robot are heavy weight, high cost and limited maneuverability.

Mori's research group [13] has developed a conceptual design for the PEACE robot for demining agricultural fields. The conceptual design of the robot is shown in Fig. 6, here uses crawler trucks to move on the ground. The robot has a large bucket on the front. Inside the bucket is a mine crusher with a metal separator. The disadvantage of this vehicle is a large weight, a small scanning area of the minefield.

An analysis of the work on the development of robots for landmine detection showed that there is a need to develop an inexpensive semi-autonomous robot installed on a vehicle capable of quick scanning of a large area of minefield and capable of marking or determining the coordinates of detected landmine.

The novelty of this work is the use of a CDPR as a landmine detection robot. In a CDPR, the end EE is suspended on flexible cables, in contrast to the rigid links in traditional parallel robots. Compared to traditional parallel robots, CDPR have lower inertial characteristics and a higher payload-to-weight ratio, which ensures high speed [14–16]. In addition, due to a wide range of use and flexibility of cables, CDPR can be used to solve complex problems with a large workspace [17, 18].

Figure 7 shows a suspended CDPR with a point-mass EE, with 3-DOF and four drive cables.

Fig. 3 Robot finder

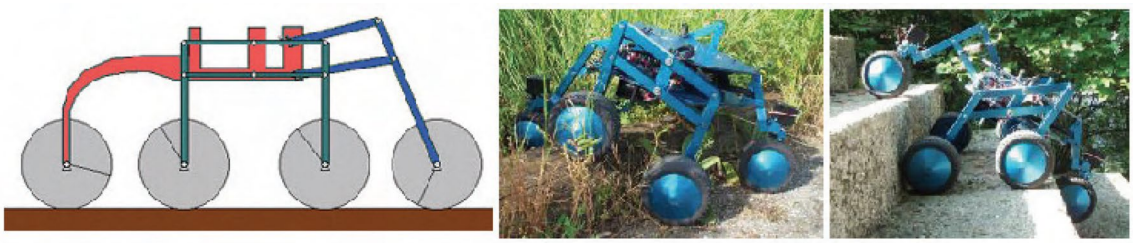

Fig. 4 The Shrimp III robot

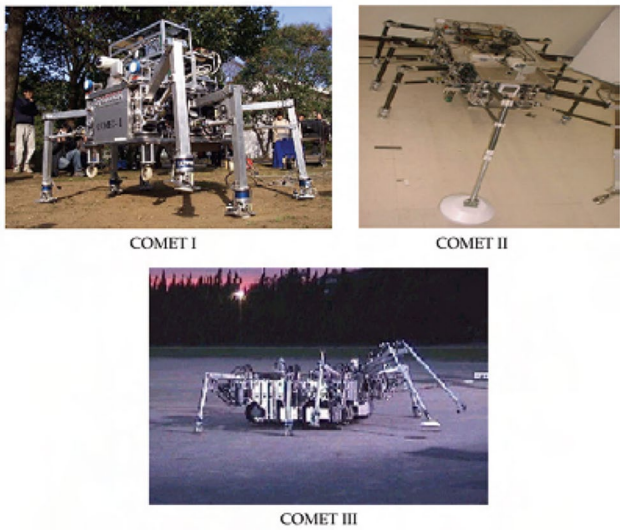

Fig. 5 Different versions of COMET

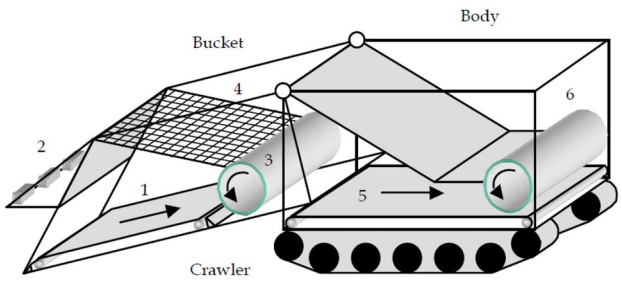

Fig. 6 Conceptual design of the PEACE robot

A feature of this CDPR configuration is that in order to maintain equilibrium, it is necessary to take into account gravity. In this configuration of the suspended CDPR, the EE is considered as a point-mass, which has only translational degrees of freedom. This assumption is correct since the dimensions of the EE are much smaller than the workspace of the CDPR. As can be seen from Fig. 7, the suspended CDPR with a point-mass EE consists of a metal

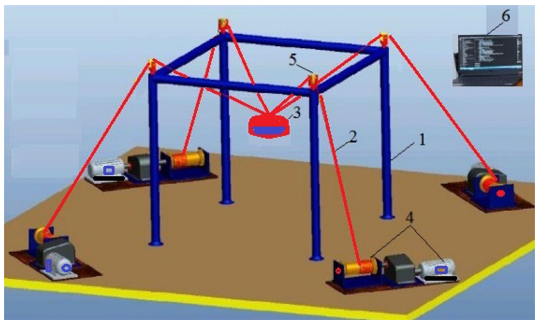

Fig. 7 A suspended CDPR

frame in the form of a rectangular parallelepiped 1, near the base of each vertical rack there are winch with servomotor 4 designed for winding (or unwinding) cables 2. The other ends of the cables 2 passing through the pulleys 5 are connected to the EE 3. The direction of rotation, as well as the speed of rotation of the winches with servomotors 4, is set by the control unit 6. Winches with servomotors 4 winding (or unwinding) cables 2 and change their length. When changing the lengths of the cables 2, the position of the EE 3 changes in the workspace of the CDPR, which is limited by the frame 1. In the design suspended CDPR with a point-mass EE, shown in Fig. 7, the EE has three translational DOF.

The paper is organized as follows. In the next section, we are designing the CDPR for landmine detection. A scheme of the CDPR for landmine detection, which installed on a vehicle, is shown. The kinematics and statics of the CDPR for landmine detection are considered. Section 3 shows experimental Setup. Prototype of the CDPR for landmine detection is shown and experimental researches are presented. In Sect. 4, conclusion is given.

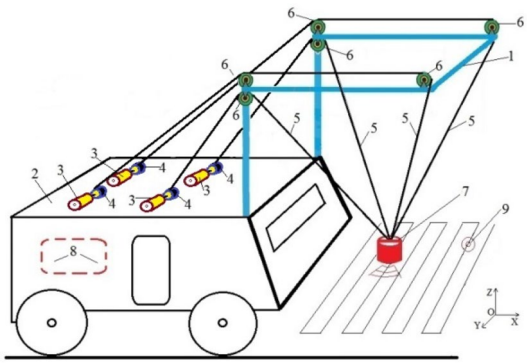

Fig. 8 Side view of the CDPR for landmine detection

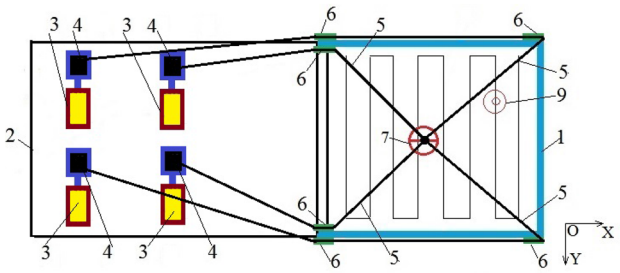

Fig. 9 Top view of the CDPR for landmine detection

2 Designing a cable-driven parallel robot for landmine detection

Figure 8 shows a side view of the CDPR for landmine detection, Fig. 9 shows a top view of the CDPR. The CDPR for landmine detection consists of a metal L - shaped space frame 1, which is rigidly fixed to the vehicle 2. On the vehicle 2, four stepper motors with winches 4 are installed, designed for winding (or unwinding) cables 5. The other ends of the cables 5 passing through the pulleys 6 are connected to the EE 7, which may contain a metal detector, a device for marking a position of a mine. The direction of rotation, as well as the speed of rotation of the stepper motors 3 with winches 4 is set by the control unit 8, which is located in the vehicle 2. In position 9, a mine is conditionally shown.

The CDPR works as follows. To search for mines 9, in the control unit 8, the law of motion of the EE 7 is set. The EE 7 has three translational degrees of freedom along the Cartesian axes X, Y, Z. From the control unit 8, control signals are sent to the stepper motors 3, which rotate the winches 4 and thereby winding (or unwinding) the cables 5 and by changing their lengths, the position of the EE 7 changes in the space of the workspace of the CDPR, which is limited by the dimensions of the frame 1. At the initial moment of time, the EE 7 is at a given height and, on command, descends possible height along the Z axis, which depends on the terrain. Then the EE, on the commands of the control unit 8, starts translational motion in the X, Y plane to detect mine 9.

The CDPR for landmine detection operates in search mode. The CDPR lowers the EE to the possible lower position and the metal detector starts scanning the minefield. When a mine is found, the location of the mine is marked with paint or its coordinates are entered into the computer. After scanning the area of the minefield, limited by the workspace of the CDPR in the X, Y plane, the information received is transmitted to the sappers.

2.1 Forward and inverse kinematics of a suspended CDPR with a point-mass EE

The kinematic scheme of the suspended CDPR with a point-mass EE is shown in Fig. 10. The following designations for the dimensions of the fixed rectangular CDPR frame are introduced: a - width, b - length, h - height. The global coordinate system O(XYZ) is set in the middle of the rectangular base of the CDPR frame, and the EE has position coordinates P(x, y, z).The distance between each vertex A, B, C, D of the cable support posts and the EE is L_i, $i = 1, 2, 3, 4$. The coordinates of the support vertex points are as follows:

A(- a/2, - b/2,h), B(a/2, - b/2,h), C(a/2,b/2,h), D(- a/2,b/2,h)

The four cable support racks are of the same height and are placed in a rectangle on the ground, if deformation is

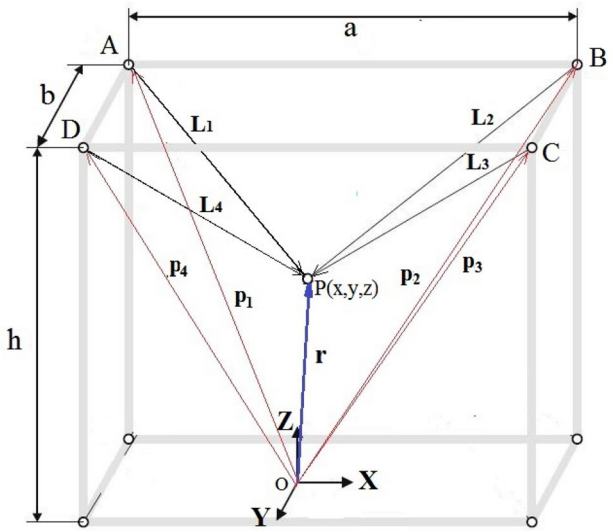

Fig. 10 The kinematic scheme of the suspended CDPR with a point-mass EE

not taken into account. To simplify the model, the cables are considered as a massless body without deformation and it is assumed that the cables are straight and stretched.

In Fig. 10, the following notations are introduced: $\mathbf{p}_i$- position vectors of points A, B, C, D attached to the fixed frame relative to the global coordinate system O(XYZ), $\mathbf{L}_i$ - cable length vector relative to the global coordinate system O(XYZ),

The equations for the inverse kinematic problem for the indicated kinematic scheme of the CDPR are presented as distances from the point P with the current coordinates x, y, z to the vertices of the quadrilateral A, B, C, D, we obtain from Fig. 10. Applying the method of closed vector contours, we obtain the following system of constraints

$$\mathbf{p}_i - \mathbf{r} - \mathbf{L}_i = 0 i = 1, \ldots, 4 \tag{1}$$

where the vector $\mathbf{r} = [x, y, z]^T \in \mathbb{R}^3$ is the Cartesian position of the end EE, relative to the global coordinate system O(XYZ). From Eq. (1) it is possible to determine the length vector of cables$\mathbf{L}_i$

$$\mathbf{L}_i = \mathbf{p}_i - \mathbf{r}, i = 1, \ldots, 4 \tag{2}$$

The scalar cable length is determined by the formula

$$L_i = \|\mathbf{p}_i - \mathbf{r}\|, i = 1, \ldots, 4 \tag{3}$$

The unit vector $\mathbf{u}_i$ along the cable has the form

$$\mathbf{u}_i = \frac{\mathbf{L}_i}{\|\mathbf{L}_i\|} \tag{4}$$

The unit vector $\mathbf{u}_i$ by convention is directed from the EE to the fixed base, which means that the positive forces are directed in the direction of decreasing the value of the length vectors $\mathbf{L}_i$ i.e. cables are shortened. To solve the forward kinematic problem of the position of the CDPR, from Eq. (3) and Fig. 10 we get

$$\begin{cases} L_1^2 = (x + \frac{a}{2})^2 + (y + \frac{b}{2})^2 + (z - h)^2 \\ L_2^2 = (x - \frac{a}{2})^2 + (y + \frac{b}{2})^2 + (z - h)^2 \\ L_3^2 = (x - \frac{a}{2})^2 + (y - \frac{b}{2})^2 + (z - h)^2 \\ L_4^2 = (x + \frac{a}{2})^2 + (y - \frac{b}{2})^2 + (z - h)^2 \end{cases} \tag{5}$$

Next, from the system of four Eq. (5), you need to choose three of them and directly calculate the position of the EE. Let's choose the equations related to the first, second and third cables, then from Eq. 5, we get the coordinates of the EE

$$\begin{cases} x = \frac{L_2^2 - L_1^2}{2a} \\ y = \frac{L_3^2 - L_1^2}{2b} \\ z = h \pm \sqrt{L_1^2 - (x - \frac{a}{2})^2 - (y - \frac{a}{2})^2} \end{cases} \tag{6}$$

where z has two solutions and in accordance with the features of the workspace of the suspended CDPR with a point-mass EE, the solution with a negative sign is correct. It should be noted that in Eq. (5) the equation for determining the length of the fourth cable is not used. The position coordinates of the EE are determined using the first three equations of system Eq. (4).

2.2 Statics of the suspended CDPR with a point-mass EE

Unlike conventional sequential or parallel robots, it is not clear whether the suspended CDPR with a point-mass EE is statically stable for a given position. In order to research the stability of various positions in which the EE can be statically balanced by cables, the mechanical balance of the EE must be taken into account. To balance the force of the EE as shown in Fig. 11, all forces acting on the EE must be taken into account. Thus, it is true

$$\sum_{i=1}^{4} \mathbf{T}_i + \mathbf{F}_p = 0 \tag{7}$$

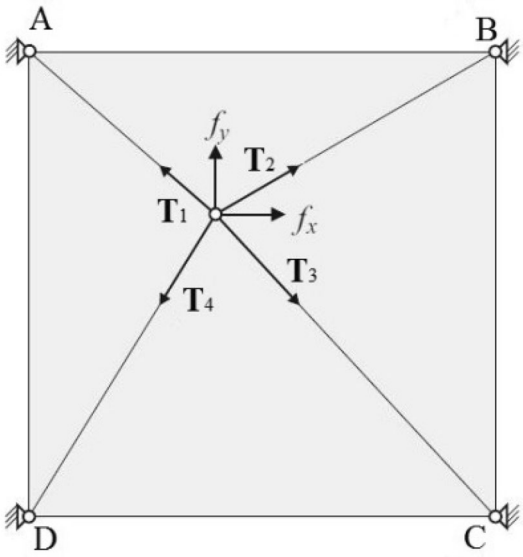

Fig. 11 Scheme of the action of forces for a CDPR with a purely translational motion

where $\mathbf{F}_\mathrm{p} = \left[f_x, f_y, f_z\right]^\mathrm{T} \in \mathbb{R}^3$ – external forces applied to the EE, $f_z = m_e g$, m_e is the mass of the EE, $\mathbf{T}_i = T_i \bullet \mathbf{u}_i$ is the tension vector of the *i*-th cable.

Here, the normal vector of the cable $\mathbf{u}_i$ is directed from the EE to the CDPR frame. From the definition of $\mathbf{u}_i$ it follows that the positive tension of the cables leads to positive values for T_i. Hence, the positive values of the tension forces of the cables cause a motion that reduces the length of the cable $\mathrm{L_i}$. We write Eq. (7) in matrix form, we obtain a linear system

$$\mathbf{A}^\mathrm{T}(\mathbf{r})\mathbf{T} + \mathbf{F}_\mathrm{P} = 0 \tag{8}$$

where $\left[T_1, T_2, T_3, T_4\right]^\mathrm{T} \in \mathbb{R}^4$, $\mathbf{A}^\mathrm{T}$ is a transposed Jacobian matrix and is called the structural matrix $\mathbf{S}$. Thus, we consider a purely force equilibrium, and the structure matrix takes the form

$$\mathbf{S} = \mathbf{A}^\mathrm{T} = \left[\mathbf{u}_1, \ldots, \mathbf{u}_4\right] \tag{9}$$

where the vectors $\mathbf{u}_i = \left[\mathbf{u}_{i,x}, \mathbf{u}_{i,y}, \mathbf{u}_{i,z}\right]^\mathrm{T} \in \mathbb{R}^3$. In Eq. 8, a number of unknown variables (m = 4) is greater than a number of equations (n = 3), so there is an infinite number of solutions for the cable tension vector $\mathbf{T}$, under the action of force $\mathbf{F}_\mathrm{P}$. In the case of m > n, [19] showed that the tension solution can be written using a pseudo-inverse matrix to invert Eq. (8) and obtain a well-known partial and homogeneous solution for the cable tension as follows:

$$\mathbf{T} = -\mathbf{S}^+\mathbf{F}_\mathrm{P} + \left(\mathbf{I} - \mathbf{S}^+\mathbf{S}^\mathrm{T}\right)\boldsymbol{Z} \tag{10}$$

where $\mathbf{S}^+ = \mathbf{S}^\mathrm{T}\left(\mathbf{S}^\mathrm{T}\mathbf{S}\right)^{-1} \in \mathbb{R}^{m\times n}$ is the pseudoinverse matrix to the structural matrix $\mathbf{S}$,$\mathbf{I} \in \mathbb{R}^{m\times n}$- identity matrix, $\mathbf{Z} = \left[z_1, z_2, \ldots, z_m\right]^\mathrm{T}$ - arbitrary column vector. In Eq. (10), the first member $\mathbf{S}^+\mathbf{F}_\mathrm{P}$ is the specific solution for the tension under the action of the force $\mathbf{F}_\mathrm{P}$. The second member $\left(\mathbf{I} - \mathbf{S}^+\mathbf{S}^\mathrm{T}\right)\boldsymbol{Z}$, which is called the homogeneous solution, is a redundancy effect that projects $\mathbf{Z}$ into the null space $\mathbf{S}$. For our suspended CDPR with a point-mass EE, the number of cables is m = n + 1. Hence, the CDPR has one degree of operation redundancy, which can be used to maintain a positive tension in each cable. Then Eq. 10 for this case looks like:

$$\mathbf{T} = -\mathbf{S}^+\mathbf{F}_\mathrm{P} + \lambda\mathbf{N} \tag{11}$$

where the homogeneous solution is now expressed as the kernel vector of the structural matrix $\mathbf{S}$, $\mathbf{N} = \left[n_1, n_2, \ldots, n_4\right]^\mathrm{T}$ multiplied by an arbitrary scalar λ. When using this method, to ensure a positive tension T_i on all cables for all possible acting forces, it is necessary and sufficient that all components of the core vector n_i have the same sign. That is, for a given point lying in the static workspace, all $n_i > 0$ or all $n_i < 0$. If one of these two conditions is met, regardless of the particular solution, the scalar λ can be found in Eq. (11). This ensures that all cable tensions T_i are positive by adding (or subtracting) a sufficiently uniform solution. Note that a strict inequality is required; if one or more $n_i = 0$, the configuration in question is not in a static workspace. In this approach (zero space approach), the kernel vector can be found using Cramer's rule. Therefore, the *i*-th zero component is the determinant of the matrix formed by deleting the *i*-th column of the structural matrix. The sign is opposite from one component to the next component. From the expression $\mathbf{S}$ in Eq. (8), the zero components can be expressed as:

$$n_i = (-1)^i \cdot \left|\mathbf{u}_1, \ldots, \mathbf{u}_4\right| \tag{12}$$

After determining the kernel vector, we need to check whether all zero components have the same sign. According to the equation

$$\sum_{i=1}^{4} |n_i| = \left|\sum_{i=1}^{4} n_i\right|, n_i \neq 0$$

After checking this condition, one can find the correct scalar λ to keep all the cables in tension. To determine the scalar λ here we use the method for estimating the tension of CDPR cables [14]. To eliminate cable slack, each component $T_i$must be greater than or equal to the specified minimum tension T_{min}. In order to obtain a guaranteed minimum positive tension in all cables, it is necessary to determineλ in each control cycle of the CDPR.

The cable tension $\mathbf{T}$ is calculated for a given force $\mathbf{F}_\mathrm{P}$ according to the equation:

$$\mathbf{T} = \begin{bmatrix} T_{p1} \\ T_{p2} \\ T_{p3} \\ T_{p4} \end{bmatrix} + \lambda \begin{bmatrix} n_1 \\ n_2 \\ n_3 \\ n_4 \end{bmatrix} \geq T_{min} \begin{bmatrix} 1 \\ 1 \\ 1 \\ 1 \end{bmatrix} \tag{13}$$

where T_{pi} are the components of a specific solution for cable tension for a given force $\mathbf{F}_\mathrm{P}$. Let's carry out the calculation for each specific component of the tension

$$\lambda_i = \frac{(T_{min} - T_{pi})}{n_i}$$

The scalar λ is defined as the maximum ofλ_i

$$\lambda = max\left\{\lambda_1, \lambda_2, \lambda_3, \lambda_4\right\}$$

The resulting value of λ should be used for all components in Eq. (11).

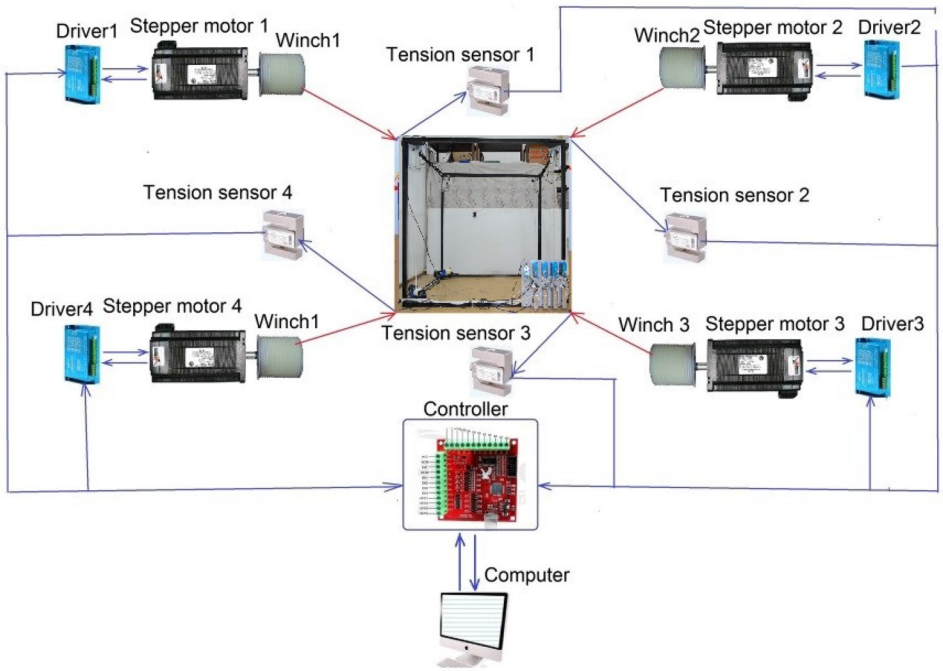

Fig. 12 The configuration of a system of prototype of the CDPR for landmine detection

3 Experimental setup

3.1 Prototype of the CDPR for landmine detection

To assemble the prototype of the CDPR for landmine detection, the configuration of its system was developed. The configuration of a system of the prototype of the CDPR for landmine detection is shown in Fig. 12. CDPR dimensions are width = 1230 mm, length = 1485 mm, height h = 1565 mm were selected for future installation on a military SUV with a width of 2000 mm, a length of 4500 mm and a height of 1500. The dimensions of the CDPR are selected in such a way as not to go beyond the overall dimensions of the vehicle.The height of the CDPR was determined from the condition of its placement on the roof of the vehicle. The mass of the EE m = 1.0 kg. Cables brand Dyneema, LIROS D-Pro 01505 – 0200, diameter 2 mm, cross-sectional area = 3.14 mm2, mass per unit length = 0.18 10 – 2 kg/m, Pulley radii of winch drums R = 40 mm. The CDPR cable drive consists of four winches with drums mounted on a shaft with two bearings at both ends. The winches are coupled to four hybrid stepper motors Nema34–86HB250-156 B with HBS86H drivers. The HBS86H drivers are connected to the Mach 3 hybrid stepper motor controller. The controller supports 4-axis control, interpolation algorithm with minimum error, high processing accuracy. Using the Mach 3 controller, the CDPR is controlled by a computer via a USB port. The tensions in the CDPR cables are determined using four tension sensor. The EE of prototype of CDPR is an XP Deus

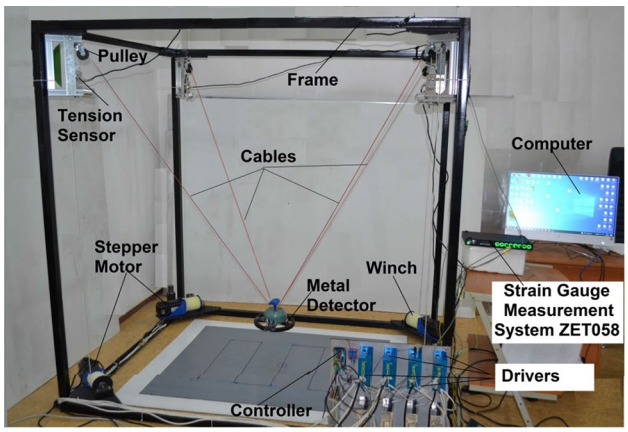

Fig. 13 The prototype of the CDPR for landmine detection

2 metal detector with a 22 cm coil. According to the developed configuration of the system of prototype of CDPR for landmine detection as shown in Fig. 12, its prototype was made as shown in Fig. 13. The prototype of the CDPR for landmine detection was developed for stationary installation in a laboratory to test its performance.

The tension sensors are connected to the ZET 058 strain gauge measuring system [20], which, together with the ZETLAB TENZO software, allows collecting information from the strain gauges in real time via eight channels simultaneously. Strain gauge measurement system ZET 058 can be used for static and dynamic measurements of loads, deformations, torque, torsional oscillations, temperature and other physical

values. Strain gauge measurement systems are represented by hardware and software suite based on multi-channel data acquisition system ZET 058 and ZETLAB TENZO software package [20].

Here we use the well-known, independent joint control (IJC), which uses a local independent PID control law in each cable to control the position of the end EE. Having the desired trajectory, cables' length can be calculated, using inverse kinematics. Then, the change in the length of each cable gives the desired angular position of related actuator using equation.

$$r_1\theta_1 = -\Delta l_i$$

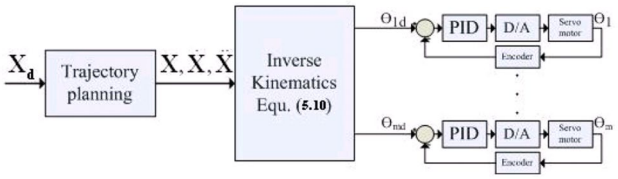

Fig. 14 Independent joint controller

This angular position should be followed by each actuator independently. Figure 14 shows the IJC controller for CDPRs which is used to move the end-EE from the current posture to the desired posture.

The IJC controller is well suited to operate CDPR for Landmine Detection and there is no need to develop a special controller (PID, adaptive, intelligent, optimal, etc.). The main task of CDPR for Landmine Detection is to scan

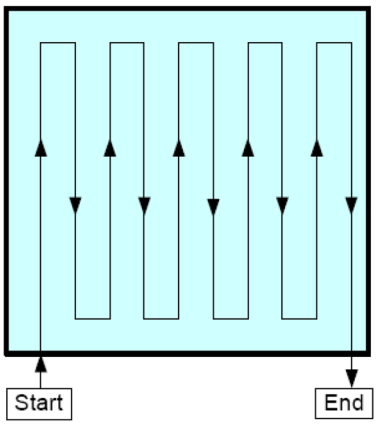

Fig. 16 The trajectory of the EE of the prototype the CDPR for landmine detection in the workspace

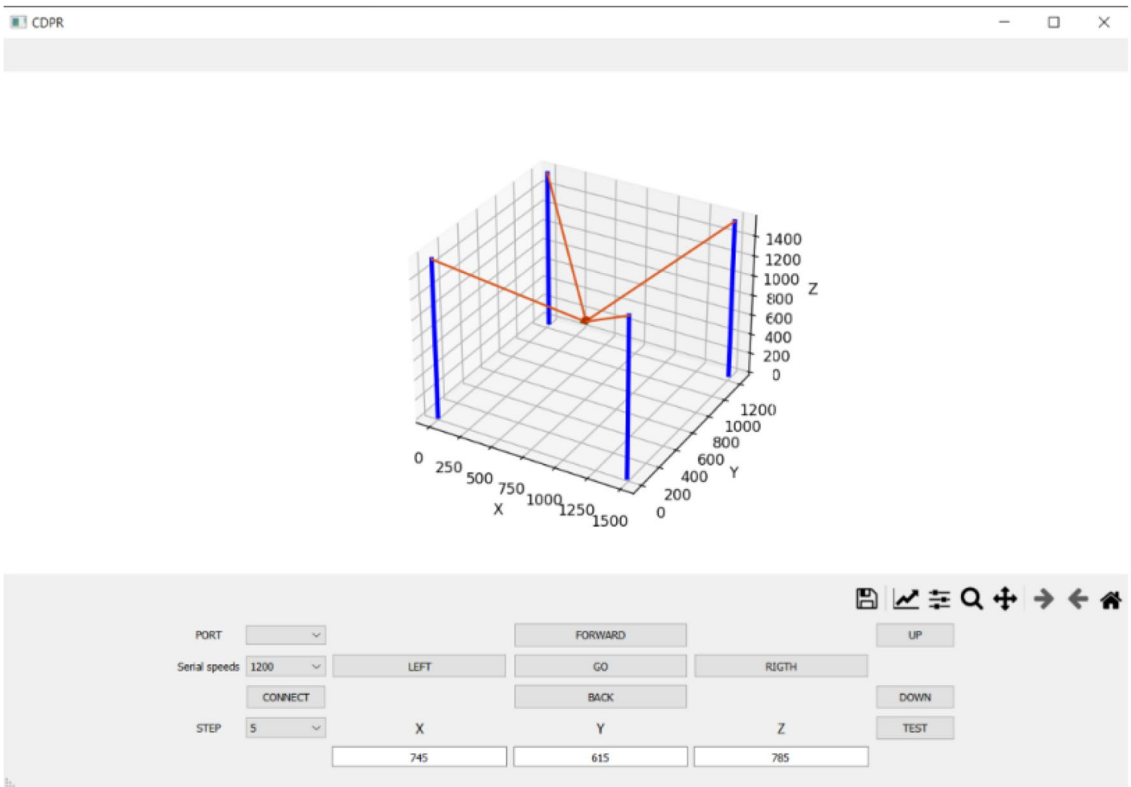

Fig. 15 Interface of the program for controlling the CDPR for landmine detection

a minefield and does not require great accuracy, and fluctuations in end EE do not affect landmine detection. Figure 15 shows the interface of the program for controlling the CDPR for landmine detection.

According to the CDPR for landmine detection control interface, we can manually control the EE. You can make manual translational motions of the EE: forward-backward, left-right, up-down. In automatic mode, the EE of the prototype a CDPR for landmine detection moves along a rectangular stepped trajectory in the robot's workspace in the XY coordinate plane, with a constant value of the coordinate along the Z axis, shown in Fig. 16. The signal

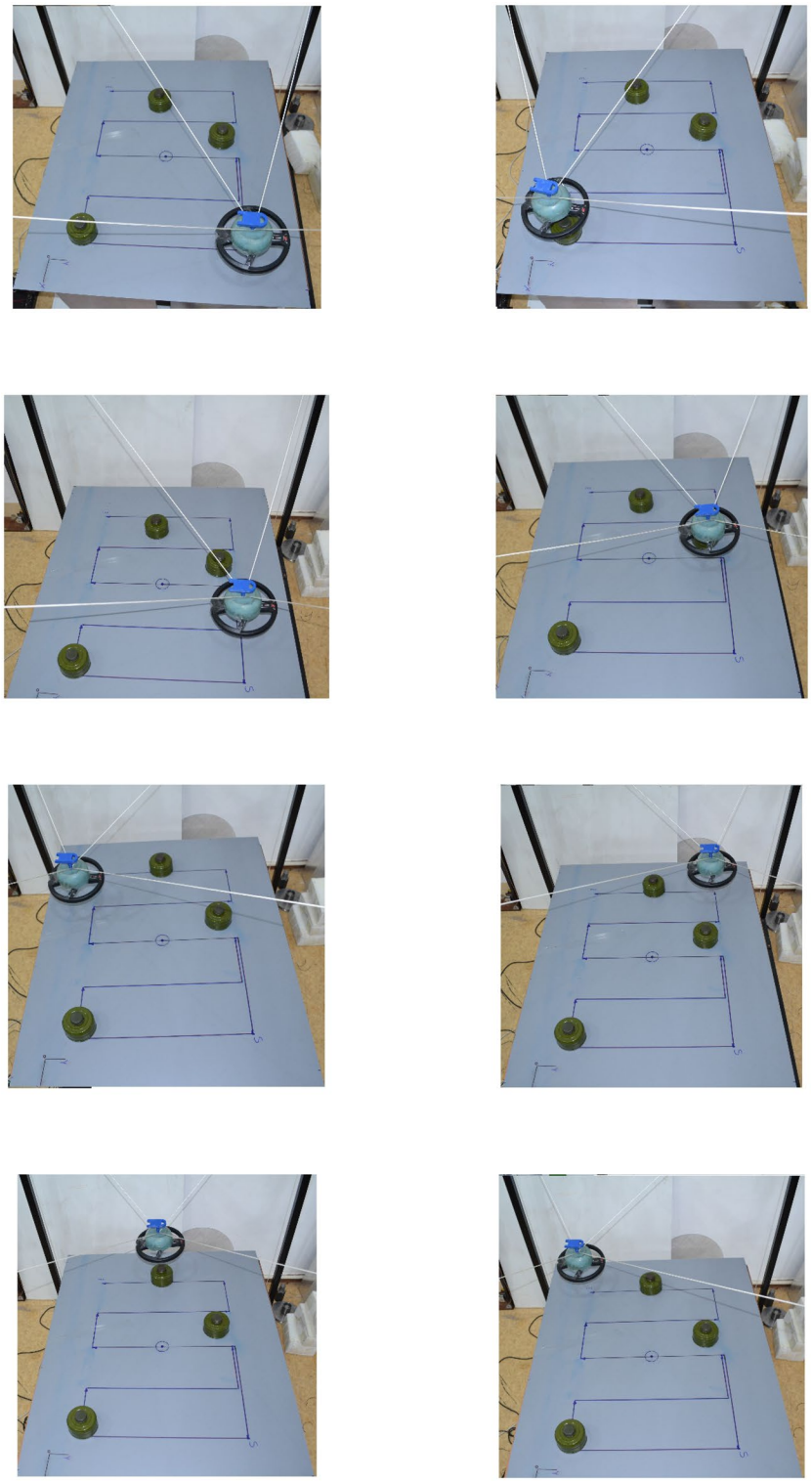

Fig. 17 The process of landmine detection by the prototype of the CDPR, top view

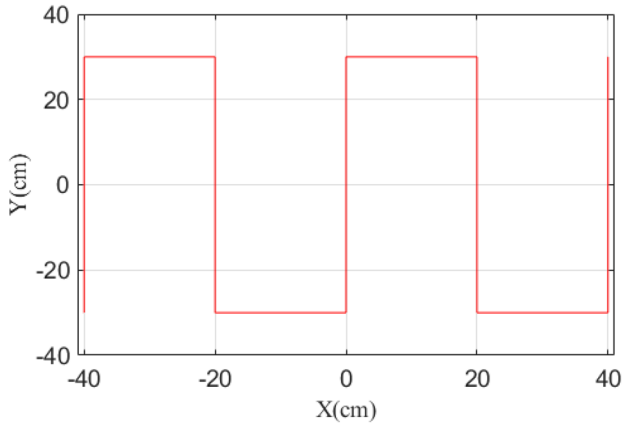

Fig. 18 Graph of a rectangular stepped trajectory of the EE of the prototype of the CDPR

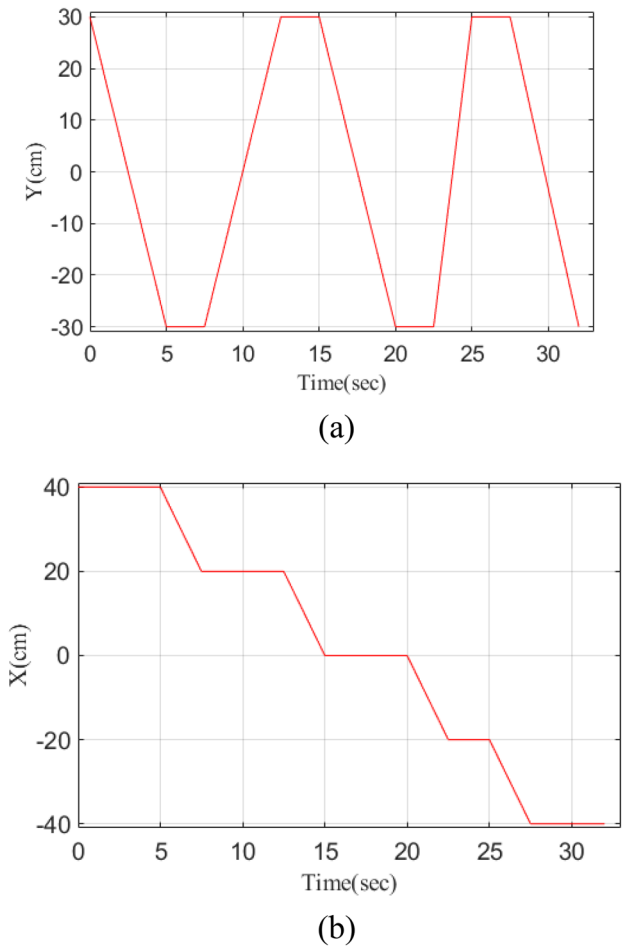

Fig. 19 Graphs of the EE trajectory: **a** along the X coordinate axis, **b** along the Y coordinate axis

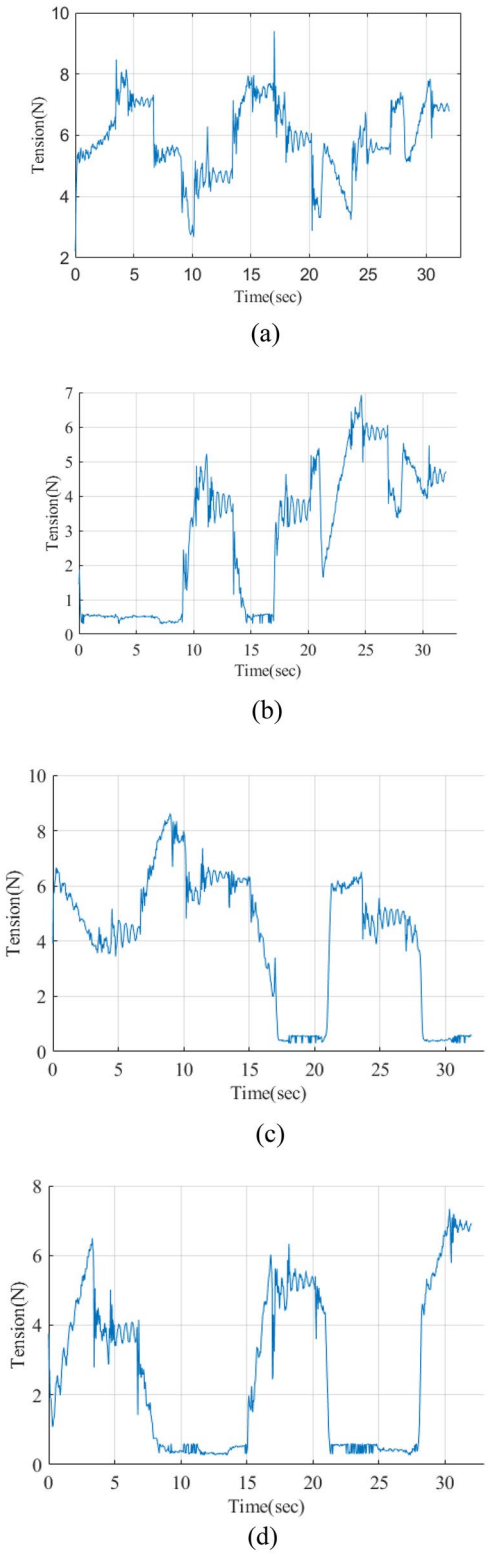

Fig. 20 Graphs of CDPR cable tensions: **a** cable 1, **b** cable 2, **c** cable 3, **d** cable 4

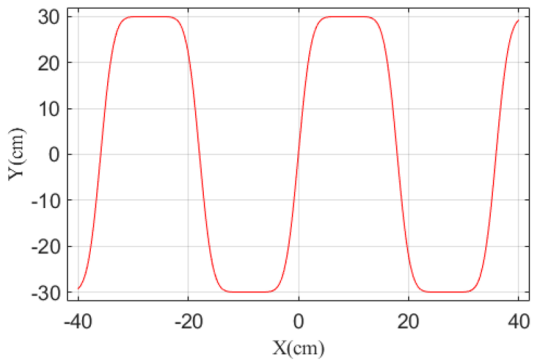

Fig. 21 Graph of the periodic function of the trajectory of the EE of the CDPR

from the metal detector when a mine is detected is transmitted to the computer, where the coordinates of the mine are stored.

Figure 17 shows the process of landmine detection by the prototype the CDPR, along a rectangular stepped trajectory, the graph of which is shown in Figs. 18 and 19.

Experimental researches were carried out to determine the tension of the cables of the prototype of the CDPR for landmine detection. Figure 20 shows the graphs of the tension of the CDPR cables in the process of landmine detection along the trajectory of EE, according to the graph (Fig. 18).

From the analysis of the graphs of the tension of the cables of CDPR with the stepped trajectory of motion of its EE, it can be seen that there are significant fluctuations and jumps in the tension of the cables. Such large fluctuations in the tension of the cables cause the buildup of EE when landmines detection. To eliminate cable tension fluctuations, it is proposed to use a smooth periodic function (14), which graph is shown in Fig. 21.

$$Y = \sin\left(\left(\frac{\pi}{2}\right) \cdot \sin\left(\left(\frac{\pi}{2}\right) \cdot \sin(X)\right)\right) \tag{14}$$

Experimental researches have been carried out to determine the tension of the cables of the prototype of CDPR for landmine detection along a new trajectory of EE. Figure 22 shows the graphs of the tension of the CDPR cables in the process of landmine detection along the trajectory of the motion of EE, according to the graph (Fig. 21).

As can be seen from the graphs in Fig. 22, cable tension fluctuations decreased, which led to more stable operation of the EE of the CDPR, when landmine detection, i.e., its buildup decreased. The use of a smooth periodic function for the trajectory of the end EE is well suited for scanning a minefield, the swing of the end EE is reduced and, most importantly, feedback is not needed.

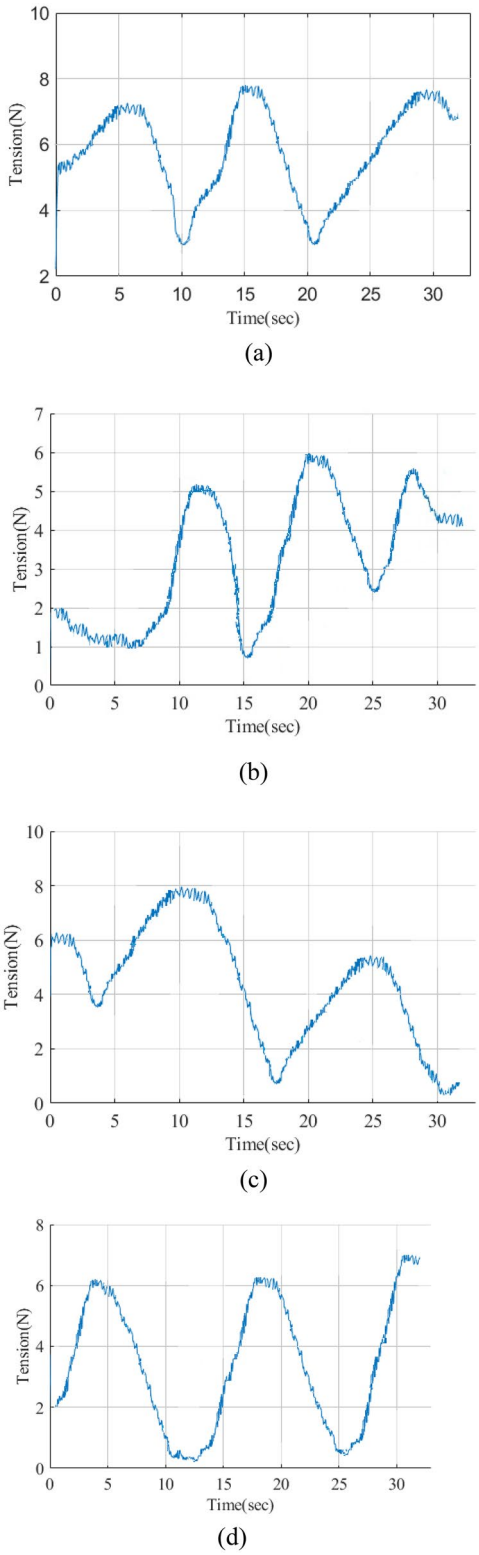

Fig. 22 Graphs of the tension of the CDPR cables along the new trajectory: **a** cable 1 **b**) cable 2 **c** cable 3 **d** cable 4

4 Conclusion

CDPR for landmine detection, mounted on a vehicle, was developed in the work. The end EE is a metal detector, which serves to detect the presence of landmine in the ground. A kinematic and static analysis of the CDPR for landmine detection is carried out. Configuration of a system of prototype of the CDPR for landmine detection has been developed. In accordance with the developed configuration of the system, CDPR for landmine detection was developed for stationary installation in laboratory to test its performance. Tests of the prototype of the CDPR for landmine detection were carried out, which showed good performance of its work for detecting landmine. Experimental researches have been carried out to determine the tension of the cables of the prototype of the CDPR for landmine detection, when its end EE moved along a stepped trajectory. An analysis of the experimental results showed that there were significant fluctuations and jumps in the tension of the cables with a stepped trajectory of the end EE of prototype of the CDPR for landmine detection. For the stable operation of the prototype of the CDPR for landmine detection, it is proposed to use smooth periodic function for the trajectory of the end EE. The use of a smooth periodic function for the scanning trajectory at the initial design stage is justified due to the fact that the scanning speed is not high. The authors plan future researches of the control system, taking into account the characteristics of servomotors, after field tests of the mine detector.

In future work, it is planned to install the prototype of the CDPR for landmine detection on a vehicle to test its operation in the field.

Author contributions Conceptualization: AJ, AT; Investigation: AJ, AK and AA; Methodology: AJ, AT; Writing: AJ, AK and AA. All authors have read and agreed to the published version of the manuscript.

Funding This research has been funded by the Science Committee of the Ministry of Science and Higher Education of the Republic of Kazakhstan (Grant No. AP09259339) and the Fundamental Research Grant (Grant Number: BR20280990) to U. Joldasbekov IME.

Declarations

Conflict of interest The authors declare that there is no conflict of interest.

References

1. Kaneko A, Fukushima E (2011) Development of an automatic landmine detection and marking system for the Demining Robot Gryphon. J Adv Comput Intell Intell Inform 15(6):737–743. https://doi.org/10.20965/jaciii.2011.p0737
2. Habib MK (2001) Mine Detection and Sensing Technologies: New Development Potentials in the Context of Humanitarian Demining. In: IEEE International Conference of Industrial Electronics, Control and Instrumentation, pp. 1612–1621. IECON 2001, USA. https://doi.org/10.1109/IECON.2001.975531
3. Nicoud JD (1996) A Demining Technology Project. In: International Conference on Detection of Abandoned Land Mines, pp.37–41. MD'96, Edinburgh, UK. https://doi.org/10.1049/cp:19961075
4. Gonzalez E, Alvarez O, Diaz Y, Parra C, Bustacara C (2005) Bsa: a complete coverage algorithm. IEEE Int. Conf. On Robotics and automation(ICRA), pp 2040–2044. Barcelona, Spain. https://doi.org/10.1109/ROBOT.2005.1570413
5. Hirose S, Kato K (1998) Development of quadruped walking robot with the mission of mine detection and removal-proposal of shape-feedback master-slave arm. In: IEEE International Conference on Robotics and Automation. pp 1713–1719. https://doi.org/10.1109/ROBOT.1998.677410
6. Nonami K, Shimoi N, Huang QJ, Komizo D, Uchida H (2000) Development of teleoperated six-legged walking robot for mine detection and mapping of mine field. In: 2000 IEEE/RSJ International Conference on Intelligent Robots and Systems, pp. 775–779. IROS 2000, Takamatsu, Japan. https://doi.org/10.1109/IROS.2000.894698
7. Rachkov MY, Marques L, De Almeida AT (2005) Multisensor Demining Robot. J Auton Robots 18(3):275–291. https://doi.org/10.1007/s10514-005-6840-y
8. Nicoud JD, Maechler P (1995) Robots for Anti-Personnel Mine Search. In: 2nd IFAC Conference on Intelligent Autonomous Vehicles, pp. 289–293. Espoo, Finland. https://doi.org/10.1016/S1474-6670(17)46987-4
9. Nonami K (2009) Development of mine detection Robot Mine Hunter Vehicle (MHV), controlled metal detector and multifunctional hydraulic manipulator. In: Furuta K, Ishikawa J (eds) Anti-personnel landmine detection for Humanitarian Demining. Springer, London. https://doi.org/10.1007/978-1-84882-346-4_8
10. Fukushima EF, Freese M, Matsuzawa T, Aibara T, Hirose S (2008) Humanitarian demining robot gryphon–current status and an objective evaluation. Int J Smart Sens Intell Syst 1(3):735–752. https://doi.org/10.21307/ijssis-2017-317
11. Estier T, Piguet R, Eichhorn R, Siegwart R (2000) Shrimp, A Rover Architecture for Long Range Martian Mission. In: The Sixth ESA Workshop on Advanced Space Technologies for Robotics and Automation (ASTRA'2000), Netherlands, http://hdl.handle.net/20500.11850/82102
12. Nonami K, Huang QJ (2003) Humanitarian mine detecting six-legged walking robot and hybrid neuro walking control with position/force control. Mechatronics 13(8):773–790. https://doi.org/10.1016/S0957-4158(03)00002-3

13. Mori Y, Takayama K, Adachi T, Omote S, Nakamura T (2005) Feasibility study on an excavation-type demining Robot. Auton Robots 18:263–274. https://doi.org/10.1007/s10514-005-6839-4
14. Pott A (2018) Cable-driven parallel Robots. Theory and application. Springer International Publishing AG, part of Springer Nature
15. Berti A, Merlet JP, Carricato M (2016) Solving the direct geometrico-static problem of underconstrained cable-driven parallel robots by interval analysis. Int J Robot Res 35(6):723–739. https://doi.org/10.1177/027836491559527
16. Zi B, Qian S (2017) Design, analysis and control of cable-suspended parallel robots and its applications. Springer Singapore, Singapore
17. Tang XQ (2014) An overview of the development for cable-driven parallel manipulator. Adv Mech Eng. https://doi.org/10.1155/2014/823028
18. Dion-Gauvin P, Gosselin C (2017) Trajectory planning for the static to dynamic transition of point-mass cable-suspended parallel mechanisms. Mech Mach Theory 113:158–178. https://doi.org/10.1016/j.mechmachtheory.2017.03.003
19. Nakamura Y (1991) Advanced Robotics - Redundancy and optimization. Addison-Wesley Publishing Company
20. ZETLAB Company. www.zetlab.com (2022) (Accesssed 2023-04-20)